Results of Micropalaeontological Analyses on Sediment Core FA09 from the Southern Red Sea Continental Shelf

Maria Geraga, Spyros Sergiou, Dimitris Sakellariou, and Eelco Rohling

Abstract

This study presents results of an examination of planktonic and benthic foraminiferal assemblages from the upper half of a 2.64 m-long sediment gravity core retrieved from the southern Red Sea continental shelf. The examined interval corresponds to the time period of the last 16 kyr. The microfaunal associations show concurrent and concomitant variations at long and short time scales. The examined deglacial interval suggests that the Strait of Bab al Mandab most likely remained open, connecting the Red Sea with the Indian Ocean, although this connection was extremely limited. Productive waters associated with inflow from the Gulf of Aden into the Red Sea prevailed during the Late Glacial and Early Holocene periods ($\sim$10 to $\sim$6 ka BP), a phase of intensified summer monsoons in the Arabian Sea. The Late Holocene period shows a reduction of productivity and sea floor oxygenation during which time the winter monsoon was stronger. Short-term variations in the abundances of planktonic and benthic foraminiferal assemblages have been linked to events of increased aridity within the Late Glacial and Holocene intervals.

M. Geraga (✉) · S. Sergiou
Laboratory of Marine Geology and Physical Oceanography, Department of Geology, University of Patras, Patras, Greece
e-mail: mgeraga@upatras.gr

D. Sakellariou
Hellenic Centre for Marine Research, 19013 Anavyssos, Athens, Greece

E. Rohling
Research School of Earth Sciences, Australian National University, Canberra, ACT 2601, Australia

E. Rohling
Ocean and Earth Science, National Oceanography Centre, University of Southampton, Southampton, SO14 3ZH, UK

1 Introduction

The Red Sea is an interesting basin from various perspectives, including geology, oceanography, biodiversity, and archaeology. It is a narrow but deep oceanic trough which is connected to the Indian Ocean through a narrow and shallow channel with a sill depth of 137 m (Biton et al. 2008) extending from the Strait of Bab al Mandab to the Hanish Sill. Today, the climate of the Red Sea is affected mostly by the Indian Ocean monsoon system (Trommer et al. 2010). These topographic and climatic signatures make the Red Sea sensitive to sea level and climatic changes, and the sediments of its seafloor are important archives preserving information regarding these changes. The glacial-interglacial signal is dominant because the full drop in sea-level during glacial maxima is of the same order as the total sill depth (Rohling et al. 1998; Siddall et al. 2003, 2004; Lambeck et al. 2011). The glacial periods with their drop in sea level are marked by the disappearance of planktonic species driven by hypersalinity, and complex reorganizations of hydrography, productivity and subsurface oxygenation in the Red Sea (Fenton et al. 2000). During interglacials, when the connection with the open sea was restored, changes in the intensity and duration of the monsoonal system affected the oceanographic patterns of the Red Sea (Arz et al. 2003; Gupta et al. 2003; Siccha et al. 2009; Trommer et al. 2010).

Topography and climate also make the Red Sea region interesting from an archaeological point of view. The southern Red Sea especially has become a focus of attention, being one of the more fertile regions of the Arabian Peninsula (Bailey et al. 2007, 2015) with a relatively narrow crossing from Africa at low sea-level stands (e.g., Rohling et al. 2013), and extensive areas of territory that are now submerged (Bailey et al. 2015). This interest underpins the DISPERSE project (Bailey et al. 2015). A critical component of this project concerns the investigation of the palaeoceanographic, palaeogeographic and palaeoclimatic evolution of the southern Red Sea, in particular in the region

of the Farasan Islands (Bailey et al. 2015, and this volume; Inglis et al., this volume; Momber et al., this volume).

Within the framework of the DISPERSE project, gravity core FA09 was retrieved from the southern Red Sea continental shelf near the Farasan Islands. Study of this undisturbed hemipelagic sediment core aims to provide new insights into the climatic and oceanographic variability in the southern Red Sea during the last glacial-interglacial cycle.

In this chapter, we present results for the upper part of the core, which spans the late glacial to Holocene interval. The core sediments were examined for variations in the abundances of planktonic and benthic foraminifera. The well-preserved record of these planktonic and benthic foraminifera in Red Sea sediments and their sensitivity to oceanographic changes make them a useful indicator of past oceanographic and climatic changes (Edelman-Fürstenberg et al. 2001; Badawi et al. 2005; Abu-Zied et al. 2011).

Geological and oceanographic setting

The Farasan Islands are located in the southern Red Sea, on the southwestern side of the Arabian Peninsula (Fig. 1). They were formed by progressive uplift due to salt diapirism, which resulted in a relative sea-level fall (Bantan 1999; Bailey et al. 2007; Demarchi et al. 2011). Ages determined from strontium and carbon isotopes suggest that this uplift is ongoing (Bantan 1999). The same regime is thought to have prevailed during the period of deposition of FA09. The low sea-level stand during the LGM (Last Glacial Maximum) resulted in exposure of the Farasan continental shelf and Pleistocene reefs around the Farasan Islands to weathering and erosion. The following sea-level rise flooded the area and left the Farasan Islands exposed. Because of local (salt-diapirism) tectonics, the relative sea-level record for the Farasan region is a complicated combination of ice-volume related eustasy (e.g., Grant et al. 2012, 2014; Lambeck et al.
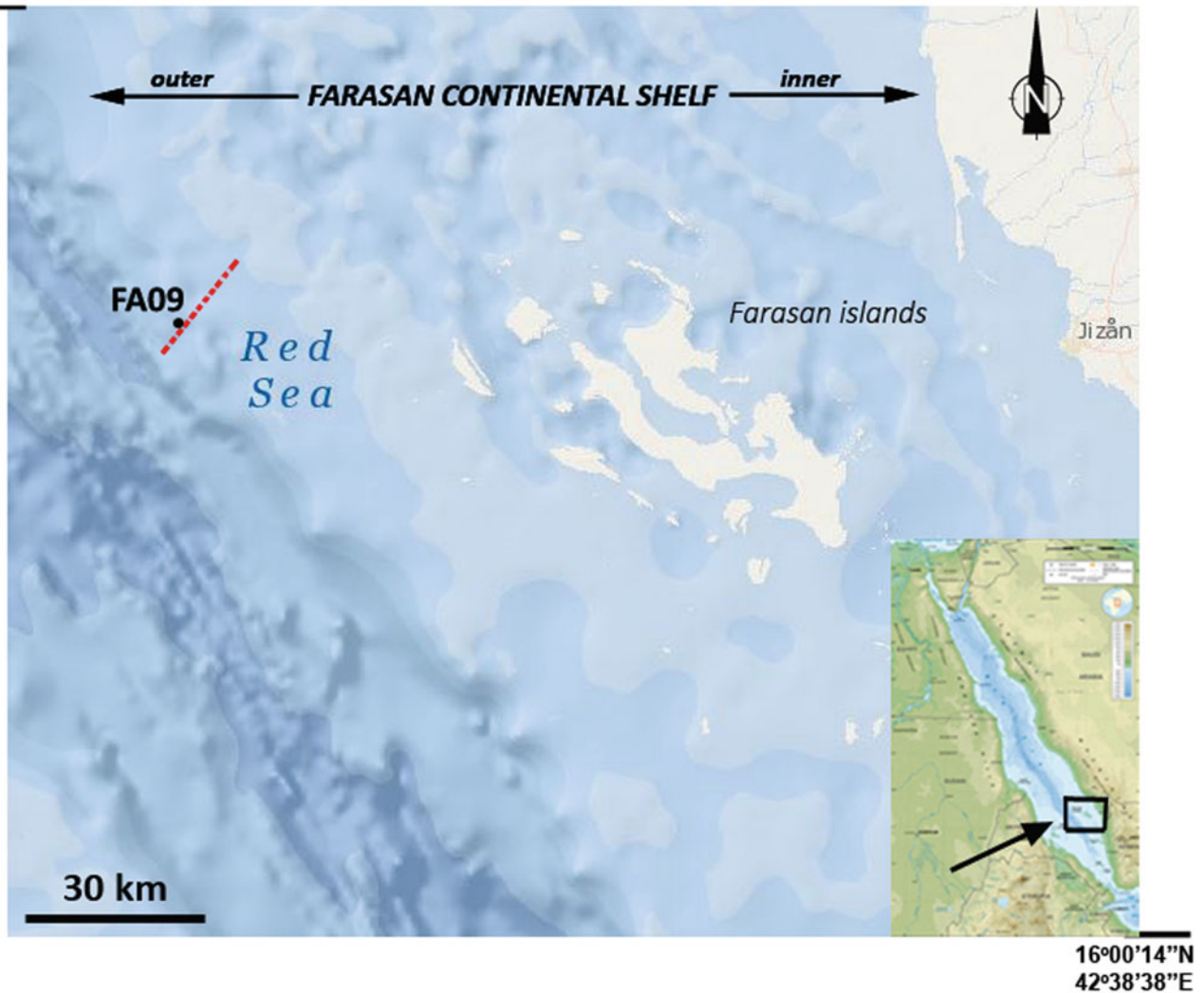
Fig. 1 Map showing the location of core FA09. The location of the seismic profile shown in Fig. 2 is marked by the dashed line
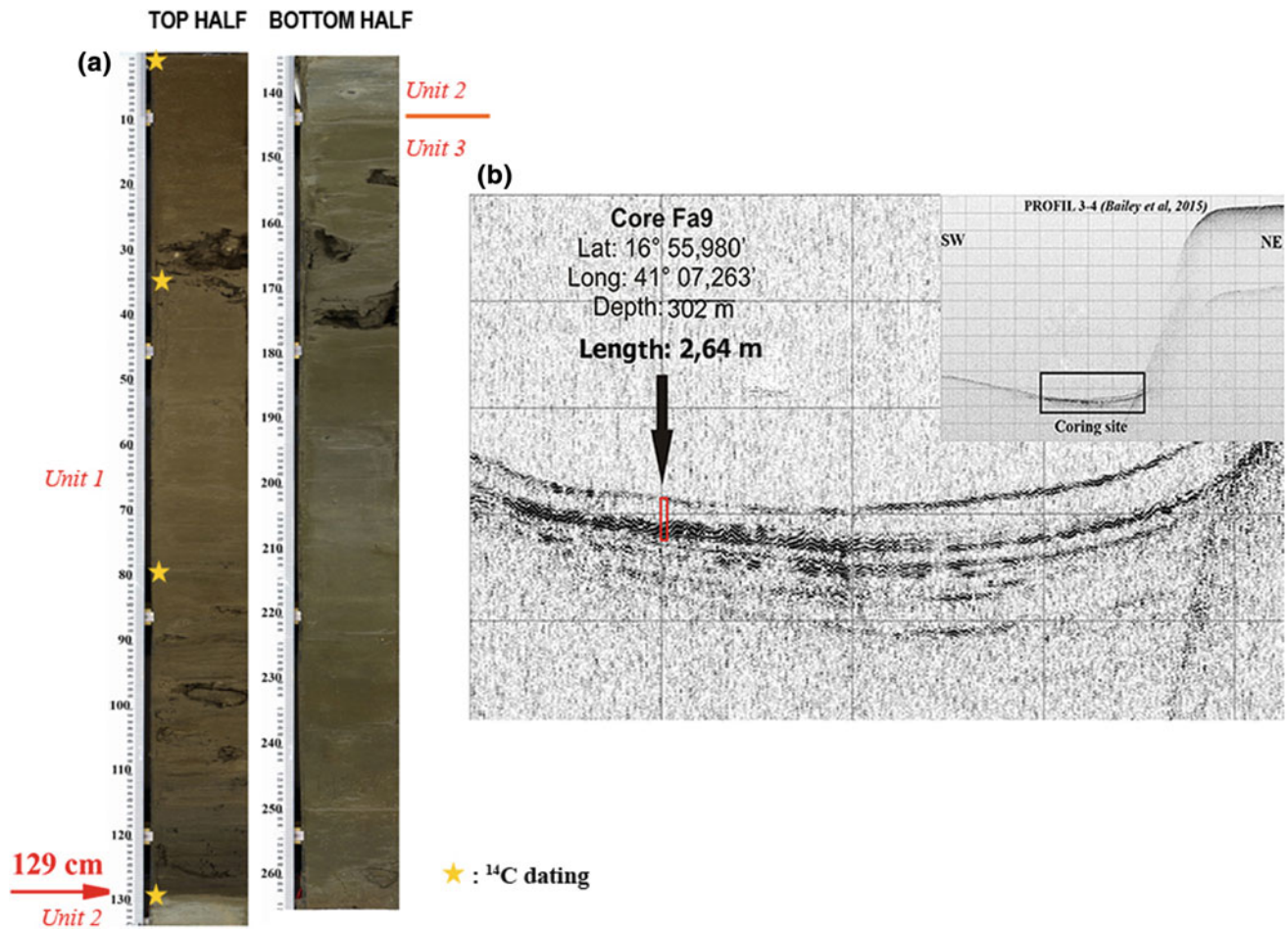
Fig. 2 **a** Photograph presenting the lithology of core FA09 (see text for lithological units 1–3). The position of radiocarbon-dated samples and the lithological change at 129 cm are marked. This work was focused on the top half; **b** Seismic profile from the coring site

2014), local uplift resulting from salt-diapirism as mentioned above, and glacio-isostatic changes related to water-loading on the wider regional shelf (e.g., Lambeck et al. 2011). In general, the (sub-) tropical climate and shallow waters lead to high production of carbonates (Abu-Zied et al. 2011), and colonization as well as proliferation of reefs.

Our core FA09 was retrieved from the outer edge of the Farasan continental shelf, which is characterized by complex topography mostly due to extensive diapirism of massive Middle to early Late Miocene evaporites, along with extensional, rift-related faulting (Bosence et al. 1998). Bailey et al. (2015) proposed that a large part of the Farasan continental shelf is occupied by a prominent, gently seaward-dipping morphological terrace developed on Pliocene-Quaternary marine limestones (Dabbagh et al. 1984; Bantan 1999), intruded by salt diapirs which derive from the afore-mentioned underlying Miocene evaporites. The same authors indicate a large number of fault-bounded basins that were potentially water-filled lakes (i.e., potentially valuable water holes) during the Pleistocene. These basins are now covered by Holocene

marine sediments. The core was collected from within one of those basins, adjoining the morphological terrace (Fig. 2).

The southern Red Sea lies under the influence of the South Asian monsoon climatic regime. Northwesterly winds dominate the area during summer and turn to southeasterly winds during winter (Morcos 1970). Oceanographic studies have shown that water exchange between the Red Sea and the Gulf of Aden (Indian Ocean) through the Bab al Mandab Strait (at the southern end of the Red Sea) is controlled by the dominant seasonal wind system (Wyrtki 1974; Woelk and Quadfasel 1996; Siddall et al. 2002; Sofianos and Johns 2007). During winter, surface water from the Gulf of Aden (GASW) enters the Red Sea moving northward, while dense, saline Red Sea water flows out into the Gulf of Aden. During summer, Gulf of Aden Interme- diate Water (GAIW) enters the basin as a subsurface layer from the Gulf of Aden (Siddall et al. 2002; Sofianos and Johns 2007). Above this layer, the Red Sea Surface Water (RSSW), which is warmer and saltier than GAIW, is moving southward. Underneath the GAIW, two Red Sea

water masses are found that both originate in the northern Red Sea: Red Sea Outflow Water (RSOW) with very high salinities (around 40 psu) and Red Sea Deep Water (RSDW) which fills the basin from about 200 m to the bottom and is characterized by very low oxygen concentrations. The sea surface temperature in the area is high (>30 °C). The salinity is also high, ranging between 36 and 41 psu throughout the water column, showing lower values in the layer associated with the GAIW mass. Oxygen concentrations vary with water depth and present two zones of minimal values, one centred at around 75 m depth (∼10 mmol/kg) associated with GAIW, and the second at around 400 m depth associated with the "old" waters of the RSDW mass. The highest oxygen concentrations occur in the surficial waters (>100 mmol/kg).

The intrusion of more nutrient-enriched waters from the Indian Ocean fuels the Red Sea ecosystem (Triantafyllou et al. 2014). During winter, the influx of nutrients and high influx of organic matter into the Red Sea from the Gulf of Aden is limited, and occurs in the surface layer. During summer, more nutrient (phosphate) and to a lesser extent TOC-enriched inflow occurs by means of the GAIW.

2   Materials and Methods

Core FA09 was collected by *R/V Aegaeo* (Hellenic Centre of Marine Research, HCMR) near the Farasan Islands (Fig. 1), within the framework of ERC-funded project DISPERSE (Bailey et al. 2015). It was obtained from 302 m water depth at 16°55.980'N, 41°07.263'E and is 264 cm long (Fig. 2a).

FA09 shows a distinct change in sedimentary characteristics (Fig. 2a). The upper unit (unit 1, 0–129 cm) consists of brownish mud with a small proportion of sand. This overlies an intermediate unit (unit 2, 129–144 cm), which consists of light grey mud and which is separated from the upper unit by a sharp contact. Then there is a lower unit (unit 3, 144–264 cm), which consists of dominant brownish mud that is sparsely interbedded with discontinuous light grey muddy laminates (Fig. 2a). We performed a number of radiocarbon assays (see below), and found that the upper 134 cm of FA09 corresponds in age to the last ∼16 kyr. These radiocarbon dates indicate a steady accumulation of marine sediments since that time to the present (Fig. 3). Because of the presence of the above-mentioned abrupt transition between unit 1 and unit 2, and uncertainty about the chronology of the intermediate and lower units, we here focus only on the upper-(marine) section of the core, that is, the latter half of the last deglaciation and the Holocene interglacial.

We took a total of fifty (50) sediment samples from the upper 134 cm, which we examined for foraminiferal populations. For the analysis, samples of wet sediment of 1 cm
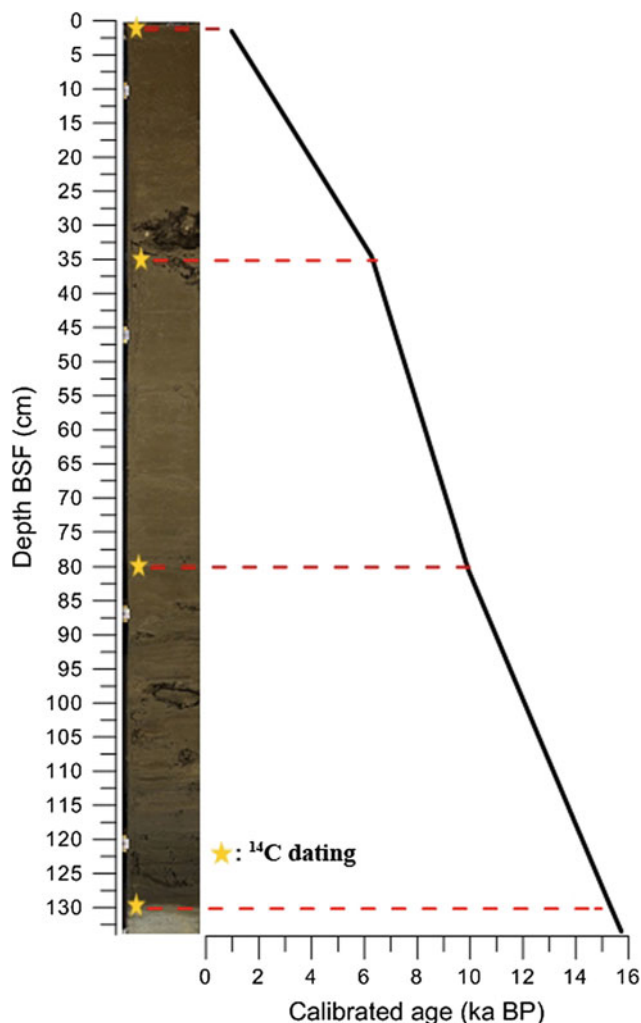
Fig. 3 The sedimentation rate as deduced from the radiocarbon dates

thickness and of specific volume were collected throughout the core. After weighing, the wet samples were dried at 50–55 °C for 24–48 h and weighed again. The samples were then washed over 63, 150 and 500 micron sieves with distilled water. An ultrasonic cleaning procedure was necessary for some samples in order to avoid coatings. Each sample from these three sieved fractions was dried at 50–55 °C for 24–48 h and weighed. In this chapter we present the results of analyses of the fraction between 150 and 500 μm.

For each sample, an aliquot containing at least 300 specimens of planktonic foraminifera was selected. Planktonic foraminifera were counted and identified up to species level. Samples with an extremely high number of foraminiferal specimens were split in appropriate aliquots by use of an Otto splitter. Benthic foraminifera were also counted and identified at least to the genus level for each sample. Species identification was mainly based on the generic classification of Loeblich and Tappan (1987) and the studies of Hottinger et al. (1993).

Each planktonic taxon is expressed as a percentage of the total assemblage and as the number of specimens per gramme of dry sediment. Each benthic taxon is expressed only as the number of specimens per gramme of dry sediment, due to low abundances of the benthic foraminifera in the aliquots (less than 200 specimens per sample). The numbers of planktonic and benthic specimens per weight of dry sediments >150 μm were estimated as indices of planktonic (PFN) and benthic (BFN) foraminiferal production, respectively. The downcore variations in planktonic percentage of the total foraminiferal assemblage (P%: (Np 100)/(Np + Nb), where Np and Nb are the number of planktonic and benthic specimens, respectively) was estimated as a quantitative index to approximate water depth (Van der Zwaan et al. 1999).

Multivariate statistical analysis (R-mode Principal Component Analysis, PCA) was carried out on the foraminiferal data in order to discriminate groups of foraminiferal species and taxa that reveal common trends and, consequently, indicate changes on the palaeoceanographic evolution. We conducted the analysis using the SPSS program (version 24). In the data set the planktic and benthic foraminifera are expressed as numbers of specimens per gram of dry sediment. Prior to multivariate statistics, rare species with extremely low contributions were omitted from the raw data set.

Four samples of about 10 mg of *Globigerinoides ruber* individuals from selected depth intervals were submitted for ^{14}C AMS analyses (Figs. 2a and 3). The analyses were carried out at the laboratories of the Scottish Universities Environmental Research Centre (SUERC). The radiocarbon results were calibrated using the Calib v.7.10 program (Table 1). The MARINE 13 curve was used and the nearest available ΔR value was selected (ΔR: 110 ± 38; Southon et al. 2002).

3 Results

3.1 Sediments

The three aforementioned lithological units of FA09 were identified on the basis of colour, grain size estimates, and sedimentary structures. The finding of fine grained sediments in the core is in agreement with the coring site's acoustic signal in geophysical surveys (Bailey et al. 2015) (Fig. 2b).

The available dates indicate that the examined part of the core (0–134 cm) corresponds to the last ∼16 kyr (Table 1), which spans the final part of Marine Isotope Stage2 (MIS2, the latter half of the deglaciation that followed the Last Glacial Maximum), and the Holocene. The mean sedimentation rate for this interval is 7.34 cm/kyr (Fig. 3). Based on this rate it is suggested that the intermediate unit may correspond to MIS2, and the lower unit to MIS3, but we do not have a robust age model for these parts, which is a concern because they are topped by a very sharp transition (discontinuity?). Hence, we focus only on the upper half of FA09.

3.2 Planktonic Foraminifera

Planktonic foraminifera are present throughout the examined interval . They show large variations in abundance, in generally low-diversity assemblages. *Globigerinoides ruber*, *Globigerinoides sacculifer*, *Globigerinella calida*, *Globigerinella siphonifera*, *Hastigerina pelagica*, *Globoturborotalita rubescens*, *Globoturborotalita. tenella*, *Orbulina universa*, *Globigerina bulloides*, *Globigerina falconensis*, *Globigerinita glutinata*, *Turborotalita clarkei*, *Turborotalita quinqueloba*, *Globorotalia menardii*, *Neogloboquadrina incompta*, *Neogloboquadrina pachyderma*, and *Neogloboquadrina dutertrei* are the main species. *Globigerinoides ruber* is the most abundant species and alone accounts for 33% on average of the total population. This species together with *G. glutinata*, *Gs. sacculifer* and *Globigerinella* spp. dominate the upper 80 cm of the core and the interval between 133 and 129 cm (at the base of the examined section) with total percentages up to 90%. At the same sediment depths, *G. bulloides* and Neogloboquadrinids contribute to the microfaunal assemblages but their numbers are increased between 80 and 129 cm, where together with *Gr. menardii* they dominate the planktonic assemblages (up to 60%) (Fig. 4).

A strong contribution of *Gs. ruber*, *G. glutinata* and *Gs. sacculifer* is common in extant planktonic foraminiferal assemblages of the region (Auras-Schudnagies et al. 1989), in recently deposited marine sediments of the Holocene in the Red Sea (e.g., Auras-Schudnagies et al. 1989; Locke and Thunell 1988; Siccha et al. 2009; Abu-Zied 2013), and in late Holocene sediments (Siccha et al. 2009; Trommer et al. 2010). This is attributed mainly to the tolerance of these species of the high sea-surface temperatures and salinities

Table 1 Radiocarbon ages and calibrated dates for the FA09 core

Sample depth BSF (cm)	Radiocarbon age BP	Calibrated date ka BP
1.5	1515 ± 32	0.95
34.5	5916 ± 32	6.23
80.5	9252 ± 32	9.91
129.5	13366 ± 56	15.33
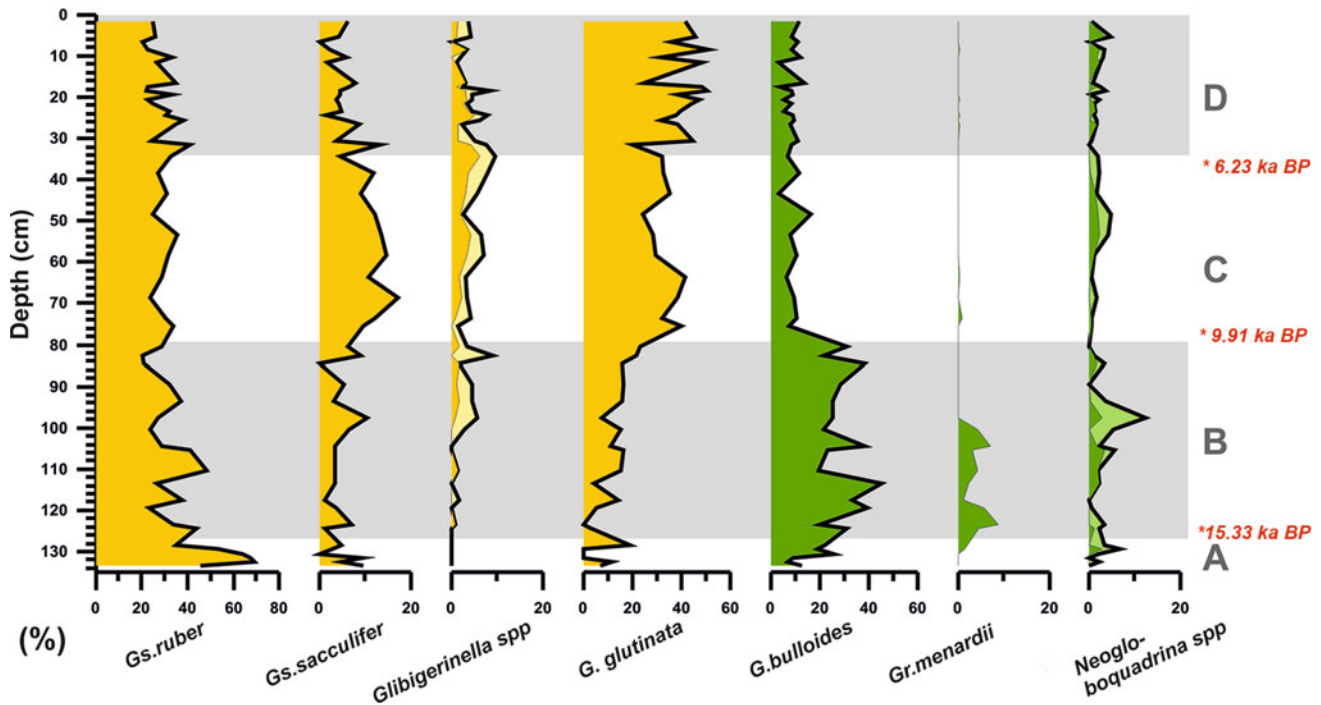
Fig. 4 Downcore variations in the abundance of planktonic forami- nifera (given in percentages of the total assemblage) through the examined interval of core FA09. The intervals A–D and the calibrated radiocarbon dates are indicated. In the diagrams for *Globigerinella* and *Neogloboquadrina*, the light-coloured areas show the abundance of *G. calida* and *N. incompta*, respectively

Table 2 Rotated factor loadings for the 5-factor model (Rotation method: Varimax with Kaiser Normalization)

Varimax rotated factor loadings					
	Component				
	1	2	3	4	5
Gs. ruber	**0.762**	0.431	0.000	–0.126	–0.201
Gs. sacculifer	**0.898**	0.009	0.077	0.077	0.080
G. glutinata	**0.848**	–0.222	–0.198	–0.095	–0.164
Globigerinella	**0.828**	–0.242	–0.212	–0.098	–0.015
G. bulloides	0.082	**0.920**	–0.020	0.017	–0.097
Gr. menardii	–0.234	**0.773**	–0.039	–0.165	–0.049
Neogloboquadrina	0.040	**0.772**	–0.155	0.065	0.095
M. millettii	–0.122	**0.826**	0.077	–0.155	0.062
Milliolids	–0.424	0.107	**0.765**	–0.121	0.109
Cibicides	–0.127	–0.254	**0.850**	0.021	0.038
Gyroidinoides soldanii	–0.069	–0.209	**0.836**	0.046	0.007
Discorbinella	–0.008	–0.034	0.098	–0.112	**0.890**
EpifaunaSum	0.021	0.325	**0.647**	0.132	0.053
Bolivina	–0.036	–0.071	0.096	**0.938**	0.102
Bulimina	–0.057	–0.104	0.037	**0.944**	0.025
InfaunaSum	0.427	–0.025	**0.560**	0.116	0.025
Agglutinants	–0.146	0.054	0.029	0.343	**0.767**

that characterize the waters of the Red Sea, and secondly to the preference of these species for low nutrient availability. Among the three species, the proportional distribution of *Gs. sacculifer* is not clear (Fenton et al. 2000; Siccha et al. 2009).

Today, the spatial distributions of *G. bulloides*, *Gr. menardii* and neogloboquadrinids present increasing trends toward the southern Red Sea; their abundances have been attributed to advection of water masses that enter from the Gulf of Aden (Auras-Schudnagies et al. 1989; Siccha et al. 2009).

3.3 Benthic Foraminifera

Benthic foraminifera are present in almost all examined samples, except for the intervals between 34 and 38 cm and at 6 cm in the core (Fig. 5). Abundances are low between 110 and 90 cm and in the upper 34 cm of the core. Although less abundant than planktonic microfauna, the benthic faunas comprise highly diverse assemblages. In total 76 benthic foraminiferal species have been identified, with *Quinqueloculina*, *Spiroloculina*, *Triloculina*, *Miliolinella*, *Bolivina*, *Bulimina*, *Cibicides*, *Discorbinella*, *Rosalina*, *Textularia*, and *Reophax* as the dominant genera.

The downcore distribution of each benthic foraminiferal taxon shows frequent variations, including intervals of disappearance of the species. Miliolids show elevated concentrations in the lower sediments between 90 and 134 cm. Above this interval, miliolids are rare or absent. High abundances of *Quinqueloculina* spp. and of general miliolids are found in oligotrophic environments and bottom waters where oxygen concentrations are sufficient (Blackwelder et al. 1996; Platon et al. 2005; Murray 2006). In addition, their abundances seem to be commonly elevated during high-salinity aplanktonic intervals in Red Sea cores (Rohling et al. 1998; Murray 1991). Epifaunal species belonging to *Amphistegina*, *Cibicides*, *Discorbis*, *Discorbinella*, *Gavelinopsis*, *Glabratella*, *Gyroidinoides*, *Millettiana*, *Neoconorbina*, *Oridosalis*, *Planorbulina* and *Rosalina* show almost concurrent appearances and abundance variations throughout the sequence. Among them *Amphistegina*, *Cibicides*, *Discorbis*, *Gavelinopsis*, *Millettiana*, *Neoconorbina*, *Planorbulina* and *Rosalina* are known as epiphytic genera and/or genera that thrive on hard substrates such as coral banks (Mateu-Vicens et al. 2010; Murray 2006). Furthermore, species belonging to *Discorbinella* and *Oridosalis* have been associated with suboxic (Kaiho 1994; Edelman-Fürstenberg et al. 2001; Murray 2006) and hypersaline bottom environments (Murray 2006; Abu-Zied et al. 2011). However, Gupta et al. (2011) consider *Oridosalis* as a genus that prefers high-oxygen conditions.

Species belonging to *Bolivina* and *Bulimina* show high abundances between 130 and 80 cm, peaking between 90 and 75 cm. Buliminid and bolivinid specimens occur in benthic assemblages of oxygen-poor and organic-rich environments (Sen Gupta and Machain-Castillo 1993; Mendes et al. 2004; Murray 2006). Specimens belonging to the infaunal genera of *Ammonia*, *Cassidulina*, *Elphidium*, *Nonion*, *Nonionella*, *Neouvigerina* and *Uvigerina* were also present in the examined samples. Their abundance in the benthic microfauna was higher between 80 and 50 cm and at the base of the core (130–134 cm).
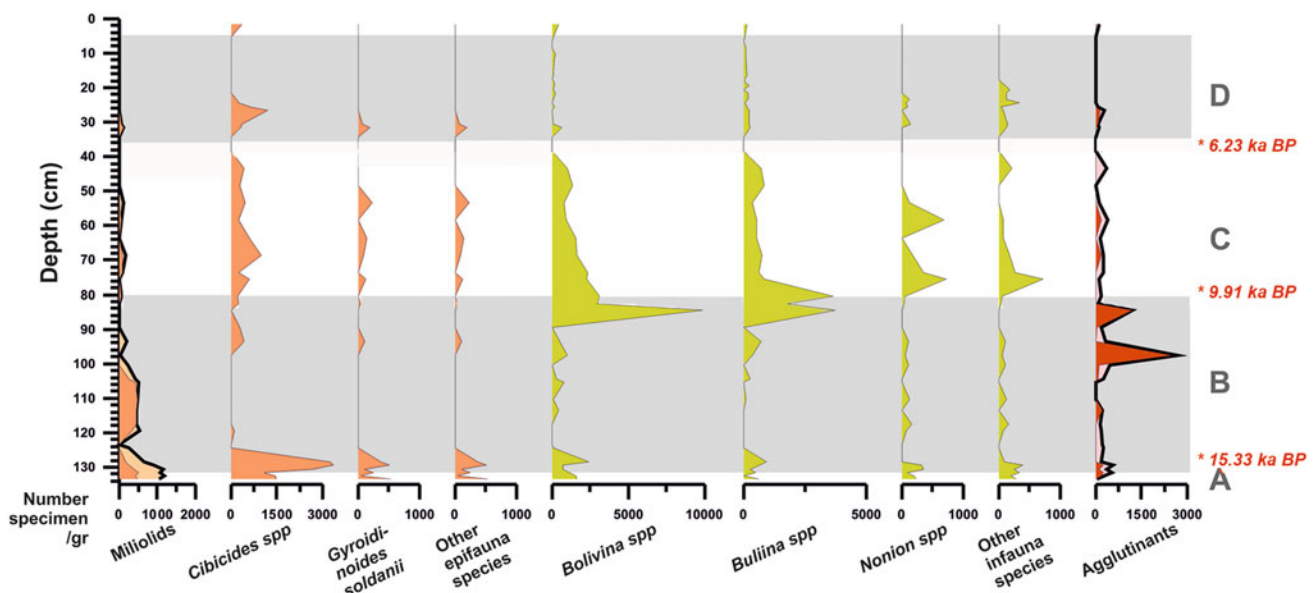
Fig. 5 Downcore variations in the abundance of benthic foraminifera (given in number of specimens per gramme of dry sediment) through the examined interval of core FA09. The intervals A–D and the calibrated radiocarbon dates are indicated. In the diagrams of miliolids and agglutinants the light-coloured areas show the abundance of *Quinqueloculina* and *Textularia*, respectively

Agglutinated benthic foraminifera belonging mostly to *Textularia* and *Reophax* showed an increased abundance at the base of the core (130–134 cm) and between 100 and 80 cm. Agglutinants are common assemblages in high-salinity environments (Abu-Zied et al. 2011; Murray 2006).

3.4 Statistical Treatment

R-mode factor analysis (PCA; Davis 1986; Reyment and Joreskog 1996) was performed using a dataset of variables representing the abundances of planktonic and benthic foraminiferal species/genera. The purpose of this analysis is to illustrate possible links and relationships between the observed planktonic and benthic foraminiferal species and genera, reducing the overall complexity of the original data and examining concurrent changes throughout the water column, thus improving our evaluation of palaeoceanographic variations. For the R-mode factor analysis, we constructed a database of seventeen variables that represent the abundances of planktonic and benthic foraminiferal species, expressed as number of specimens per unit weight of dry sediment (>150 µm). The variable *Globigerinella* includes the sum of *G. calida* and *G. siphonifera* (Weiner et al. 2015) and the variable *Neogloboquadrina* represents the sum of all species belonging to *Neogloboquadrina* genera (*N. incompta*, *N. pachyderma*, *N. duertrei*, *N. humerosa*). In the benthic assemblages, the group labeled *Epifauna Sum* includes the sum of *Discorbis*, *Neoconorbina*, *Planorbulina*, and *Rosalina*, while the group labeled *Infauna Sum* includes the sum of *Ammonia*, *Cassidulina*, *Elphidium*, *Neouvigerina* and *Nonion*. In order to select the most suitable factor model, a combination of criteria was followed. These criteria include total variance estimation, Catell's scree test and factor loading values (see Davis 1986; Reyment and Joreskog 1996). The final number of selective factors found is five. These five factors explain 76% of the total variance and each variable shows communalities higher than 0.5 (Table 2). This means that the 5-factor model expresses sufficiently the analyzed variables. The first two factors represent relations between planktonic foraminiferal taxa (including the benthic species *Millettiana millettii* in the second factor), while the next three indicate relations between the benthic foraminiferal taxa.

Factor 1 explains the largest proportion (23%) of the total variance and has high positive loadings for *Gs. ruber*, *Gs. sacculifer*, *G. glutinata* and *Globigerinella*. Open ocean observations show that *Globigerinoides ruber*, *Gs. sacculifer* and *Globigerinella* thrive in the upper water column, up to 200 m water depth, where the temperature ranges between 11 and 32 °C and the salinity ranges between 22 and 49 psu (Fenton et al. 2000, and references therein). *Globigerinita glutinata* shows a more cosmopolitan character (Fenton et al. 2000, and references therein) and is an indicator of SW monsoon variations in the open-ocean upwelling area of the Arabian Sea (Anderson and Prell 1991). Based on the above, we interpret the assemblage of Factor 1 as an indicator of warm surface waters of high salinity, while the oxycline (if any) is at least below the depth of reproduction of these species (80–100 m; Fenton et al. 2000, and references therein).

Factor 2 explains a significant proportion (20%) of the total variance and has high positive loadings for *G. bulloides*, *Neogloboquadrina*, *Gr. menardii* and the Cymbaloporidae *M. millettii*. *Globigerina bulloides* is typical of regions of increased productivity (Thiede 1975; Overpeck et al. 1996; Siccha et al. 2009). Today this species is found only in the southern Red Sea and the Gulf of Aden (Auras-Schudnagies et al. 1989; Siccha et al. 2009) and is thought to reflect an influence of upwelling of nutrient-rich deep water toward the surface layer (Kroon and Ganssen 1989) in response to strong monsoon activity (Gupta et al. 2003). As this upwelling progresses, neogloboquadrinids and *Gr. menardii*—which are usually abundant at a deeper level in the water column—appear in abundance in the early stages, while *G. bulloides* appears to thrive during the final stage (Kroon and Ganssen 1989). In addition, Gupta et al. (2010) documented that, in the Indian Ocean, benthic species belonging to Cymbaloporidae are found as indicators of productive surface waters following the trends of *G. bulloides.* Thus, we interpret the assemblage of Factor 2 as an indicator of productive waters associated with upwelling of nutrient-enriched deep waters to the surface.

Factor 3 explains 14% of the total variance and has high positive loadings for miliolids, the groups of *Epifauna Sum* and *Infauna Sum* and *G. soldanii*. In the present central Red Sea, species belonging to genera such as *Cibicides*, *Gyroidinoides*, and *Neouvigerina* occur at the margin or below the Oxygen Minimum Zone (OMZ) in bottom environments with well oxygenated conditions (1–2.5 ml O_2/l) and moderate to low organic fluxes (2.5–0.8 g C/m^2/yr), and moderate to low Total Organic Carbon (TOC) content ranging from 0.3 to 0.1 wt% (Edelman-Fürstenberg et al. 2001). Elevated oxygen levels are also implied by the miliolids (Blackwelder et al. 1996; Platon et al. 2005). Based on the above, we interpret the assemblage of Factor 3 as an indicator of oligotrophic to mesotrophic conditions and a well oxygenated seafloor.

Factor 4 explains 12% of the total variance and has high positive loadings for buliminids and bolivinids. In the present central Red Sea, species belonging to *Bolivina* and *Bulimina* genera occur in the centre of the OMZ (Oxygen Minimum Zone) where the oxygen concentrations are low (<0.5 ml O_2/l) and the organic carbon flux and TOC content are high (~3.5 g C/m^2/y and 0.7 wt%, respectively; Edelman-Fürstenberg et al. 2001). In addition, species belonging to these genera are recorded in the Arabian Sea where enhanced

surface primary production leads to high organic flux on the seafloor with low to intermediate oxygen conditions (De and Gupta 2010). Based on the above, we interpret the assemblage of Factor 4 as an indicator of eutrophic seafloor levels and moderate to low oxygen conditions.

Factor 5 explains 8% of the total variance and has high positive loadings for *Discorbinella* and agglutinants. Today agglutinants (together with miliolids) dominate hypersaline lagoons in the Red Sea (Abu-Zied et al. 2011). Furthermore, taxa such as *Textularia* show an affinity to dysoxic and hypoxic conditions and to increases in salinity (Moodley et al. 1998; Almogi-Labin et al. 1996). In addition, *Textularia agglutinans* is found in the OMZ in the Arabian Sea (De and Gupta 2010). *Discorbinella* is a major component in the centre of the OMZ in the central Red Sea (together with *Bolivina* and *Bulimina*; Edelman-Fürstenberg et al. 2001). Thus, we interpret the assemblage of Factor 5 as an indicator of low oxygen and likely high salinity bottom conditions.

Figure 6 shows downcore variations of the factor scores for each factor.

4 Discussion

Our results for core FA09 allow us to recognize four environmentally distinct intervals in the southern Red Sea within the last 16 ka:

Interval A (15.7–15.3 ka BP, base of the examined core interval). This interval is characterized by extremely low numbers of planktonic foraminifera (PFN) and high scores on factors 3 and 5 (Fig. 6).

Intervals where the planktonic foraminifera are almost absent ("aplanktonic" zones) have been previously recorded in sediment cores from the Red Sea, and they have been attributed mainly to the prevalence of extremely high sea surface salinity (about 50 psu or higher) due to near-isolation of the Red Sea at low full-glacial sea levels (Almogi-Labin et al. 1991; Fenton et al. 2000, and references therein). The youngest of these intervals occurred at the Last Glacial Maximum (LGM, or MIS2). Interval A corresponds to the late stages of this period. The presence of planktonic foraminiferal species in FA09 suggests that salinity in the study area did not rise to levels beyond the tolerance of these microorganisms. This is in agreement with observations from other cores from the southernmost Red Sea, which do not show "truly" aplanktonic layers (Fenton et al. 2000, and references therein). These microfaunal associations within the "aplanktonic" interval are different relative to the central and northern Red Sea in terms of foraminiferal population and diversity (Fenton et al. 2000). This can be ascribed to advection of specimens from the Gulf of Aden through the Bab el Mandab Strait.

This layer in FA09 therefore supports the notion that water-exchange through the strait remained active during at least the late phase of the LGM, as was also inferred by Rohling et al. (1998), (Fenton et al. 2000); Siddall et al. (2003); and Fernandes et al. (2006). Any separation from the Indian Ocean in this interval would not only have resulted in immediate aplanktonic conditions, but also in drawdown of the Red Sea water level below the sea-floor depth of FA09 within a century or two, with associated evaporite deposition. Instead, we see continuous low-abundance planktonic foraminiferal faunas.

Although high salinity may have had an influence as well (see above), the low P% values (Fig. 6) suggest that the core location was much shallower than it is today and was probably part of the inner shelf (Van der Zwaan et al. 1999; Murray 1991). The co-occurrence of high scores of factors 3 and 5 indicates that miliolids and agglutinants were dominant components in the benthic microfauna (Figs. 5 and 6). Similar associations occur in hypersaline lagoons in the present Red Sea close to the core site (Abu-Zied et al. 2011). Furthermore, similar assemblages have been obtained during glacial intervals in marine cores in previous studies (Locke and Thunell 1988; Badawi et al. 2005). This suggests the establishment of low oxygen and high salinity conditions in waters over the seafloor during the late phase of the LGM in the southern Red Sea (Locke and Thunell 1988; Fenton et al. 2000, and references therein). It also confirms that, while the Strait of Bab al Mandab may have remained open, it did become seriously restricted, causing high salinities in the basin (see also Locke and Thunell 1988; Rohling et al. 1998; Fenton et al. 2000; Fernandes et al. 2006).

This interval ends with an increase in the BFN numbers associated with high scores of factor 3 (Fig. 6), suggesting an improvement of sea-floor oxygenation and reduction in salinity in association with post-glacial sea-level rise. Similar trends have been seen in benthic microfaunas at the end of the LGM interval in other cores from the southern and central Red Sea (Badawi et al. 2005).

Interval B (15.3–10 ka BP). This interval corresponds to the latest glacial period and onset of the Holocene. It is characterized by high PFN values and high scores of factors 2 and 3 (Fig. 6).

The high abundance of planktonic foraminifera may be explained by improvements in the water exchange over the Hanish Sill, from the Arabian Sea into the Red Sea, as sea level rose (Rohling et al. 1998; Siddall et al. 2003). Today the intrusion of relatively fresh, cold and nutrient-enriched waters from the Gulf of Aden constitutes the major source of nutrients in the southern Red Sea (Raitsos et al. 2015). It is likely that the sea level of this time-interval, which was still low and therefore created a shallow strait in the south, permitted only a two-layered water exchange between inflow
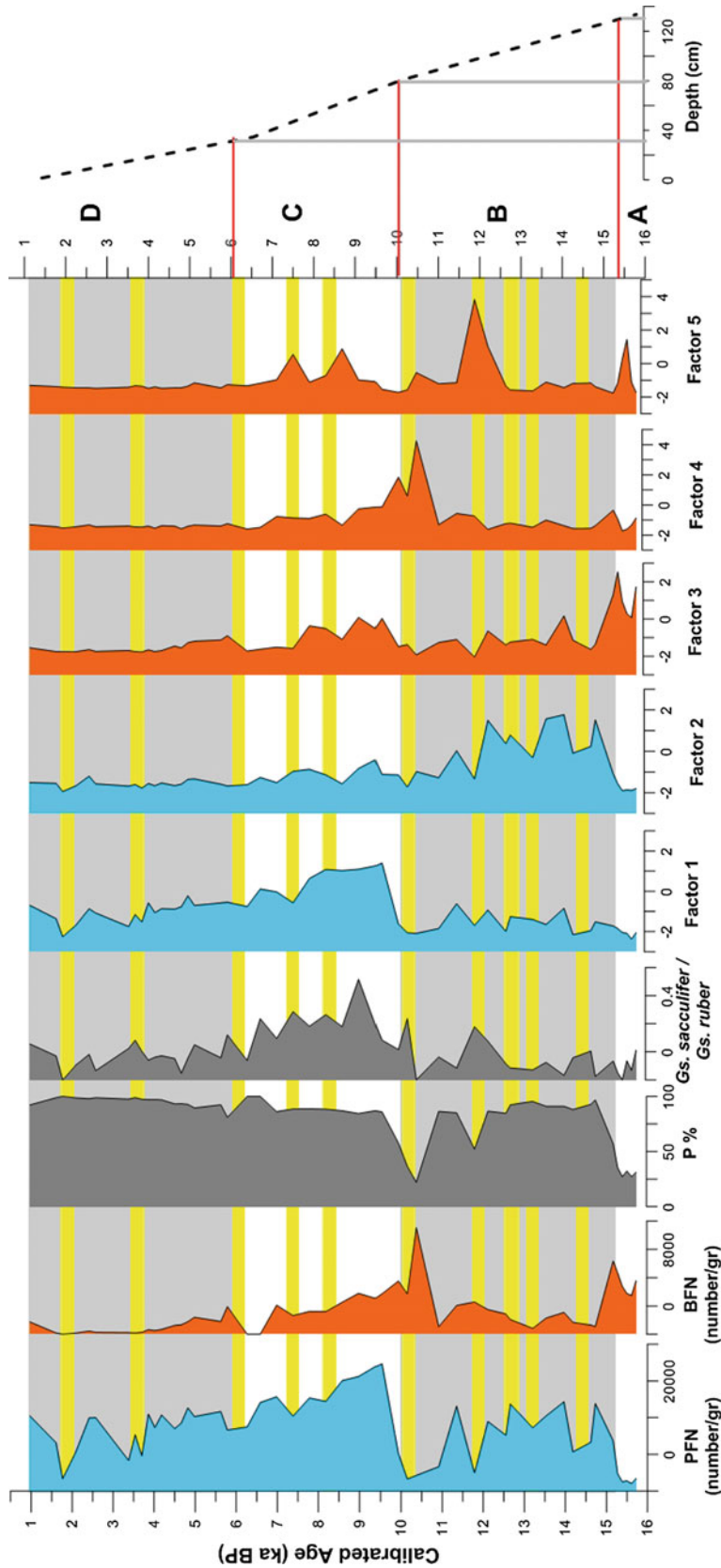
Fig. 6 Chronostratigraphy and downcore variations in the abundance of benthic and planktonic foraminifera (given in number of specimens per gramme of dry sediment) together with the percentage participation of planktonic forams (P%) and *Gs. sacculifer* versus *Gs. ruber* abundances, and the downcore variations of the scores of factors 1–5. The age-depth correlation is depicted. The intervals A–D and intermediate time periods discussed in the text are indicated

from the Gulf of Aden and outflow from the Red Sea (Siddall et al. 2002). The core site was situated in shallower waters than today, where coastal upwelling could have developed. Today coastal upwelling—which induces local productivity—is observed in the shallow zone of the Farasan Archipelago (Sofianos et al. 2016; Dreano et al. 2016). The relatively shallow inflow of Gulf of Aden waters of time-interval B, along with this potential development of local coastal upwelling, would have increased productivity in the southern Red Sea, leading to an increase of the planktonic assemblages of factor 2 (high factor 2 scores; Figs. 4 and 6). At the same time, the abundance of deeper-dwelling planktonics together with high factor-3 scores and moderate factor-4 values (Figs. 4 and 6) suggest that the water column above the site of FA09 was sufficiently oxygenated throughout and that mesotrophic conditions had been established on the seafloor.

Within this interval, short-term perturbations are observed in the abundance of the planktonic population, which is dominated by the factor-2 assemblage. The most pronounced changes are observed at around 14.5 ka and 11.5 ka BP, as brief reductions in the planktonic populations. Today, the ecosystem and the oceanographic conditions in the southern Red Sea are more prone to impacts from the Indian Ocean than other parts of the Red Sea (Sofianos and Johns 2007; Triantafyllou et al. 2014). Therefore, we propose that the short-term changes in FA09 may be linked to changes in the Arabian Sea. Marine palaeoclimatic, palaeo-productivity and denitrification records from the Arabian Sea suggest that the intensity of the summer SW monsoon was stronger during interstadials and weaker during stadials, within the last glacial cycle (e.g., Schulz et al. 1998; Ivanochkoa et al. 2005). The stronger SW monsoon caused stronger upwelling in the Arabian Sea during both the Holocene and interstadials, enhancing fluxes of buried organic matter in the area and reducing the water-column oxygenation. On the contrary, the LGM and the stadials were times of reduced organic burial fluxes and improved water-column oxygenation in the Arabian Sea (Ivanochkoa et al. 2005). The intermittent Interval-B reductions in planktonic populations in core FA09, and in particular in species related to eutrophic waters, likely reflect weakened inflow of subsurface Gulf of Aden water due to reduced SW-monsoon-driven upwelling in the Gulf of Aden. This reduced the nutrient availability at the site of core FA09. Almogi-Labin et al. (1991) have also documented temporal changes in the planktonic fauna of the central Red Sea (foraminifera and pteropods) during this time-interval (Late Glacial period). Almogi-Labin et al. (1991) attributed these changes to oscillations between humid and arid conditions, where arid conditions produced unfavourable conditions for survival of the organisms. From the present study, it seems that oceanographic conditions in the southernmost Red Sea never reached sufficiently severe

conditions to cause total absences of planktonic populations, as seen in more northern parts of the Red Sea at this time. However, it is noticeable that the event, at around 11.5 ka coincides with an increase of the factor 5 scores (Fig. 6), implying a reduction in seafloor oxygen concentration and an increase in salinity that coincided with the harsher conditions that prevailed in more northern parts of the Red Sea. A comprehensive explanation for all combined signals remains elusive in the absence of detailed dating, but it is evident that some coherent pattern existed across the basin.

The end of interval B is marked by an increase of factor-4 scores (Figs. 5 and 6). The abundances of buliminids and bolivinids increase sharply at around 10.5 ka and remain high in the subsequent interval, which implies an increase in the organic flux on the sea floor and/or a reduction of seafloor oxygenation at the core site. This may be explained by an onset of strong GAIW intrusion into the Red Sea. At around 10.5 ka BP, sea level had risen sufficiently (to ~50 m below the present level) to allow the intrusion of the GAIW over the Hanish sill (Siddall et al. 2002, 2003). A three-layer water exchange was established and remained active until the present. It is likely that at 10.5 ka, the onset of GAIW inflow with significant quantities of nutrients and organic matter increased productivity and thus the organic fluxes on the seafloor in the southern Red Sea, and so increased the abundances of buliminids and bolivinids at FA09.

Interval C (10–6 ka BP). The main characteristics of this interval are increased planktonic abundances and high factor-1 scores (Fig. 6). Moderate factor-3 scores suggest that, within this interval, the seafloor was mesotrophic and sufficiently oxygenated (Fig. 6).

A sharp increase of planktonic populations related to warm and salty surface waters (factor 1) reflects the establishment of warm and salty surface conditions at the site of FA09 in the early Holocene. Planktonic assemblages reflecting warm, high salinity and oligotrophic waters similarly developed throughout the Red Sea in the early Holocene (Siccha et al. 2009; Trommer et al. 2010). We propose that flooding of the vast Red Sea shelves (doubling the sea's surface area) when sea-level rose higher than about –50 m may have caused some of this shift to predominance of species indicative of warm, salty, and oligotrophic conditions. In these assemblages, variations in the relative abundances between individual species have been attributed to changes in salinity and productivity along the Red Sea. These variations were not simultaneous between the northern and central Red Sea and they are attributed to differentiations in the water circulation mode of the Red Sea (Siccha et al. 2009; Trommer et al. 2010), and relatively larger shelf areas in the south than in the north may also have played a role.

The onset of the PFN-increase and of increases in the abundances of *Gs. ruber*, *Gs. sacculifer*, *G. glutinata*

(Figs. 5 and 6) at ∼10 ka in FA09 closely coincide with similar variations in the central Red Sea (core KL09; Siccha et al. 2009; Trommer et al. 2010), suggesting a synchronicity between the central Red Sea and the region of FA09. However, in detail the planktonic assemblages show some dissimilarities between these regions. The most pronounced is the (low-abundance) contribution of productivity-indicator species (factor 2) in FA09, and their absence in the central Red Sea. We propose that this is related to GAIW influences that were present at this time only in the southern Red Sea region of FA09.

The early Holocene is a known period of increased monsoon intensity and northward migration of the Intertropical Convergence Zone (ITCZ; Fleitmann et al. 2007, and references therein). The strong summer monsoons of that time caused intensified upwelling of nutrient-enriched waters in the Arabian Sea (Ivanochkoa et al. 2005; Gupta et al. 2011), which included increased upwelling of nutrient-enriched GAIW in the Gulf of Aden. This facilitated enhanced GAIW (and nutrient) penetration into the Red Sea. Today, in summer, the GAIW is observed in the southern Red Sea at depths between 50 and 100 m (Sofianos and Johns 2007). Although its properties are strongly diluted northward, the main part of the GAIW intrusion can reach up to ∼16°N (only ∼100 km south of FA09), where it is detected mainly as a mass of low salinity (37–38 psu), elevated nutrient concentrations (higher than 10 μmol/l) and a dissolved oxygen content of 22.5 mmol/kg, at ∼75 m depth (Sofianos and Johns 2007 Dreano et al. 2016). With intensified monsoon circulation and increased GAIW penetration during the early Holocene, we suggest that our observed planktonic foraminiferal changes indicate that the site of FA09 came under the direct influence of the enhanced GAIW intrusion. The resultant productivity increase is further reflected by increases of buliminids and bolivinids in the benthic assemblage, which are related to increased organic fluxes to the seafloor (factor 4; Figs. 5 and 6). Indeed, this assemblage peaks between 10.5 and 8 ka, almost in phase with the most intense monsoon period (Fleitmann et al. 2007). Given that these specific planktonic and benthic assemblages are seen in FA09 and not in the central Red Sea (Siccha et al. 2009), we infer that the location of FA09 was close to the northernmost edge of the early Holocene GAIW intrusion.

Comparison between the planktonic assemblages of FA09 and those of the central Red Sea reveals some further interesting differences. Notably, Gs. Sacculifer (Fig. 6), is the dominant species in the central and northern Red Sea, where its abundance exceeds that of Gs. ruber during the early Holocene (Siccha et al. 2009; Trommer et al. 2010). In the southern Red Sea (core FA09), however, Gs. sacculifer shows elevated numbers (Fig. 4) but does not exceed Gs. ruber (see ratio Gs. sacculifer versus Gs. ruber; Fig. 6). Although open-ocean observations show that both Gs. ruber and Gs.

sacculifer dominate surficial waters of high temperature and high salinity (Fenton et al. 2000, and references therein), there are studies which show Gs. sacculifer as a relatively stenohaline species and Gs. ruber as a euryhaline species (Hemleben et al. 1987; Bijma et al. 1990). In addition, Gs. sacculifer seems to dominate oligotrophic areas but Gs. ruber dominates water masses of higher productivity (Halicz and Reiss 1981; Bijma et al. 1990). If temperature and salinity control the proportional distribution of Gs. sacculifer, then this difference should be explained by the contribution of the water from the Gulf of Aden in the southern Red Sea. Today, the inflow of water from the Gulf of Aden at the surface in the winter and subsurface in the summer affects the southern Red Sea (FA09) and provokes surface waters of lower salinity and higher productivity in comparison to the surface water of the northern parts of the Red Sea. If this oceanographic pattern was the same during the early Holocene, then the differences in the relative abundance of Gs. sacculifer observed between the southern Red Sea and the northern parts of the Red Sea could reflect the prevalence of less saline and more fertile waters above the site of core FA09.

Both the typical planktonic and benthic populations show progressive reductions toward the end of interval C at 6 ka (Fig. 6), suggesting a gradual increase in salinity and food-availability stress in surface waters, and a resultant decrease in organic flux to the seafloor.

Interval D (6–1 ka BP). The main characteristics of this interval, which corresponds to the late Holocene, consist of a reduction in planktonic populations (low PFN numbers, low scores of factors 2 and 3), and low benthic foraminiferal abundances (low BFN).

Interval D contains similar planktonic foraminiferal species to interval C, but at lower abundances for almost all species (Figs. 4 and 6). Among them, Gs. sacculifer shows the largest reduction. This decline of this species coincides with a near-absence of the factor-4 benthic assemblage (Figs. 5 and 6). In addition, for a time-interval between 4.0 and 2.0 ka, benthic populations almost completely disappear, which suggests a complete lack of food availability (or, alternatively, anoxic bottom waters, for which we have no further indications). Together, these observations suggest a prevalence of less eutrophic waters, relative to the preceding interval (C). The late Holocene is marked by shorter and weaker summer monsoon circulation and southward migration of the ITCZ (Fleitmann et al. 2007, and references therein). Trommer et al. (2010) also observed changes in the microfauna associations between 3.7 and 1.7 ka in the central and northern Red Sea, which they attributed to weakening summer monsoons along with intensification of winter monsoons. In addition, an intensification of the OMZ (Oxygen Minimum Zone) and weakening of upwelling in the Arabian Sea during the Late Holocene also reflect weakening summer monsoons (Das et al. 2017). The above

suggests that the inferred reduction in nutrient availability in this interval (D) of FA09 may be related to weakening of the GAIW inflow into the Red Sea.

5   Conclusions

Four intervals were distinguished, based mainly on variations in the planktonic foraminiferal assemblages and benthic foraminiferal abundances in the sequence of core FA09. These intervals correspond to the upper part of MIS2, the Late Glacial and the early to late Holocene. The examined interval of MIS2 suggests that the Strait of Bab al Mandab most likely remained open during the LGM, albeit in a very restricted form. During the Late Glacial, initiation of coastal upwelling and of inflow from the Gulf of Aden into the Red Sea resulted in more productive conditions in the southern Red Sea. It is likely that significant inflow of GAIW started at around 10.5 ka. From that time onward, the planktonic and benthic microfauna at the site of FA09 reflect changes in the southern Red Sea that followed changes in the intensity of (summer) monsoon winds. During the Late Glacial and early Holocene, the water column was in general well oxygenated throughout, but during the late Holocene a reduction of productivity and oxygen levels occurred during which time the winter monsoon was stronger. Temporal and simultaneous variations between the various proxies investigated seem linked to a combination of sea-level and monsoon influences on the Red Sea in general, and in its southernmost sector in particular (where FA09 is located) through modulation of GAIW inflow through the Strait of Bab al Mandab.

References

Abu-Zied RH (2013) Effect of the Red Sea brine-filled deeps (Shaban and Kebrit) on the composition and abundance of benthic and planktonic foraminifera. Arab J Geosci 6:3809–3826

Abu-Zied RH, Bantan RA, Basaham AS, El Mamoney MH, Al-Washmi HA (2011) Composition, distribution, and taphonomy of nearshore benthic foraminifera of the Farasan Islands, southern Red Sea, Saudi Arabia. J Foramin Res 41:349–362

Almogi-Labin A, Hemleben C, Meischner D, Erlenkeuser H (1991) Paleoenvironmental events during the last 13,000 years in the central Red Sea as recorded by pteropoda. Paleoceanography 6:83–98

Almogi-Labin A, Hemleben C, Meischner D, Erlenkeuser H (1996) Response of Red Sea deep-water agglutinated foraminifera to water mass changes during the Late Quaternary. Mar Micropaleontol 28:283–297

Anderson DM, Prell WL (1991) Coastal upwelling gradient during the Late Pleistocene. In: Proceedings of the ODP Scientific Results, vol 117, pp 265–276

Arz HW, Lamy F, Pätzold J, Müller PJ, Prins M (2003) Mediterranean moisture source for an Early Holocene humid period in the northern Red Sea. Science 300:118–121

Auras-Schudnagies A, Kroon D, Ganssen G, Hemleben C, van Hinte JE (1989) Distributional pattern of planktonic foraminifers and pteropods in surface waters and top core sediments of the Red Sea, and adjacent areas controlled by the monsoonal regime and other ecological factors. Deep Sea Res Part A 36:1515–1533

Badawi A, Schmiedl G, Hemleben C (2005) Impact of late Quaternary environmental changes on deep-sea benthic foraminiferal faunas of the Red Sea. Mar Micropaleontol 58(1):13–30

Bailey G, Al-Sharekh A, Flemming N, Lambeck K, Momber G, Sinclair A, Vita-Finzi C (2007) Coastal prehistory in the southern Red Sea Basin, underwater archaeology, and the Farasan Islands. In: Proceedings of the Seminar for Arabian Studies, vol 37, pp 1–16

Bailey G, Deves MH, Inglis RH, Meredith-Williams MG, Momber G, Sakellariou D, Sinclair AGM, Rousakis G, Al Ghamdi S, Alsharekh AM (2015) Blue Arabia: Palaeolithic and underwater survey in SW Saudi Arabia and the role of coasts in Pleistocene dispersals. Quat Int 382:42–57

Bailey G, Meredith-Williams M, Alsharekh A, Hausmann N (this volume) The archaeology of Pleistocene coastal environments and human dispersals in the Red Sea: Insights from the Farasan Islands

Bantan RA (1999) Geology and sedimentary environments of Farasan Bank (Saudi Arabia) southern Red Sea: A combined remote sensing and field study. Unpublished PhD dissertation, University of London, U.K., 296 pp

Bijma J, Faber J, Hemleben C (1990) Temperature and salinity limits for growth and survival of some planktonic foraminifers in laboratory cultures. J Foraminiferal Res 20(2):95–116

Biton E, Gildor H, Peltier WR (2008) The Red Sea during the Last Glacial Maximum: Implications for sea level reconstruction. Paleoceanography 23, PA1214. https://doi.org/10.1029/2007pa001431

Blackwelder P, Hood T, Alvarez-Zarikian C, Nelsen TA, McKee B (1996) Benthic foraminifera from the NECOP study area impacted by the Mississippi River plume and seasonal hypoxia. Quat Int 31:19–36

Bosence DWJ, Al-Awah MH, Davison I, Rosen BR, Vita-Finzi C, Whittaker E (1998) Salt domes and their control on basin margin sedimentation: a case study from the Tihama plain, Yemen. In: Purser BH, Bosence DWJ (eds) Sedimentation and tectonics in Rift Basins: Red Sea-Gulf of Aden. Chapman and Hall, London, pp 448–466

Dabbagh A, Emmermann R, Hötzl H, Jado AR, Lippolt HJ, Kollmann W, Moser H, Rauert W, Zötl JG (1984) The development of Tihamat Asir during the Quaternary. In: Jado AR, Zotl JG (eds) Quaternary Period in Saudi Arabia, vol 2. Sedimentological, Hydrogeological, Hydrochemical, Geomorphological, Geochronological and Climatological Investigations in Western Saudi Arabia. Springer, Vienna, pp 150–173

Das M, Singh RK, Gupta AK, Bhaumik AK (2017) Holocene strengthening of the Oxygen Minimum Zone in the northwestern Arabian Sea linked to changes in intermediate water circulation or Indian monsoon intensity? Palaeogeogr Palaeoclimatol Palaeoecol 483:125–135

Davis JC (1986) Statistics and data analysis in geology. Wiley, New York, p 647

De S, Gupta AK (2010) Deep-sea faunal provinces and their inferred environments in the Indian Ocean based on distribution of Recent benthic foraminifera. Palaeogeog Palaeoclimat Palaeoecol 291:429–442

Demarchi B, Williams MG, Milner N, Russell N, Bailey G, Penkman K (2011) Amino acid racemization dating of marine shells: amound of possibilities. Quat Int 239:114–124

Dreano D, Raitsos DE, Gittings J, Krokos G, Hoteit I (2016) The Gulf of Aden Intermediate Water intrusion regulates the southern Red Sea summer phytoplankton blooms. PLoS ONE 11(12):e0168440. https://doi.org/10.1371/journal.pone.0168440

Edelman-Fürstenberg Y, Scherbacher M, Hemleben C, Almogi-Labin A (2001) Deep-sea benthic foraminifera from the central Red Sea. J Foramin Res 31:48–59

Fenton M, Geiselhart S, Rohling EJ, Hemleben C (2000) Aplanktic zones in the Red Sea. Mar Micropaleontol 40:277–294

Fernandes C, Rohling EJ, Siddall M (2006) Absence of Quaternary Red Sea land bridges: biogeographic implications. J Biogeogr 33:961–966

Fleitmann D, Burns S, Mangini A, Mudelsee M, Kramers J, Villa I, Neff U, Al-Subbary A, Buettner A, Hippler D, Matter A (2007) Holocene ITCZ and Indian monsoon dynamics recorded in stalagmites from Oman and Yemen (Socotra). Quat Sci Rev 26:170–188

Grant KM, Rohling EJ, Bar-Matthews M, Ayalon A, Medina-Elizalde M, Bronk Ramsey C, Satow C, Roberts AP (2012) Rapid coupling between ice volume and polar temperature over the past 150 kyr. Nature 491:744–747

Grant KM, Rohling EJ, Bronk Ramsey C, Cheng H, Edwards RL, Florindo F, Heslop D, Marra F, Roberts AP, Tamisiea ME, Williams F (2014) Sea-level variability over five glacial cycles. Nat Commun 5:5076. https://doi.org/10.1038/ncomms6076

Gupta AK, Anderson DM, Overpeck JT (2003) Abrupt changes in the Asian southwest monsoon during the Holocene and their links to the North Atlantic Ocean. Nature 421:354–357

Gupta AK, Sarkar S, De S, Clemens SC, Velu A (2010) Mid-Brunhes strengthening of the Indian Ocean Dipole caused increased equatorial East African and decreased Australasian rainfall. Geophys Res Lett 37:L06706, 6

Gupta AK, Mohan K, Sarkar S, Clemens SC, Ravindra R, Uttam RK (2011) East-west similarities and differences in the surface and deep northern Arabian Sea records during the past 21 Ka. Palaeogeog Palaeoclimat Palaeoecol 301:75–85

Halicz E, Reiss Z (1981) Palaeoecological relations of foraminifera in a desert enclosed sea: the Gulf of Aqaba. Mar Ecol 2:15–34

Hemleben C, Spindler M, Breitinger I, Ott R (1987) Morphological and physiological responses of Globigerinoides sacculifer (Brady) under varying laboratory conditions. Mar Micropaleontol 12:305–324

Hottinger L, Halicz E, Reiss Z (1993) Recent Foraminifera from the Gulf of Aqaba, Red Sea. Slovenska Akademija Znanosti in Umetnosti, Ljubljana, p 179

Ivanochkoa TS, Ganeshrama RS, Brummerb GJ, Ganssenc G, Jungc S, Moretond S, Kroon D (2005) Variations in tropical convection as an amplifier of global climate change at the millennial scale. Earth Planet Sci Lett 235(1):302–314. https://doi.org/10.1016/j.epsl.2005.04.002

Kaiho K (1994) Benthic foraminiferal dissolved-oxygen index and dissolved oxygen levels in the modern ocean. Geology 22:719–722

Kroon D, Ganssen G (1989) Northern Indian Ocean upwelling cells and the stable isotope composition of living planktic foraminifers. Deep-Sea Res 36:1219–1236

Lambeck K, Purcell A, Fleming NC, Vita-Finzi C, Alsharekh AM, Bailey G (2011) Sea level and shoreline reconstructions for the Red Sea: Isostatic and tectonic considerations and implications for hominin migration out of Africa. Quat Sci Rev 30:3542–3574

Lambeck K, Rouby H, Purcell A, Sun Y, Sambridge M (2014) Sea level and global ice volumes from the Last Glacial maximum to the Holocene. Proc Natl Acad Sci USA 111(43):15296–15303

Locke S, Thunell RC (1988) Paleoceanographic record of the last glacial/interglacial cycle in the Red Sea and Gulf of Aden. Palaeogeog Palaeoclimat Palaeoecol 64:163–187

Loeblich AR, Tappan H (1987) Foraminiferal genera and their classification, vol 2. Van Nostrand Reinhold, New York

Mateu-Vicens G, Box A, Deudero S, Rodriguez B (2010) Comparative analysis of epiphytic foraminifera in sediments colonized by seagrass Posidoniaoceanica and invasive macroalgae Caulerpa spp. J Foramin Res 40:134–147

Mendes I, Gonzalez R, Dias JMA, Lobo F, Martins V (2004) Factors influencing recent benthic foraminifera distribution on the Guadiana shelf (southwestern Iberia). Mar Micropaleontol 51:171–192

Momber G, Sakellariou D, Bailey G, Rousakis G (this volume) The multi-disciplinary search for underwater archaeology in the southern Red Sea

Moodley L, Schaub BEM, Van der Zwaan GJ, Herman PMJ (1998) Tolerance of benthic foraminifera (Protista: Sarcodina) to hydrogen sulphide. Mar Ecol Prog Ser 169:77–86

Morcos SA (1970) Physical and chemical oceanography of the Red Sea. Oceanogr Mar Biol Ann Rev 8:73–202

Murray JW (1991) Ecology and paleoecology of benthic foraminifera. John Wiley & Sons, New York, p 397

Murray JW (2006) Ecology and applications of benthic foraminifera. Cambridge University Press, pp 426

Overpeck J, Rind D, Lacis A, Healy R (1996) Possible role of dust-induced regional warming in abrupt climate change during the last glacial period. Nature 384:447–449. https://doi.org/10.1038/384447a0

Platon E, Sen Gupta BK, Rabalais NN, Turner RE (2005) Effect of seasonal hypoxia on the benthic foraminiferal community of the Louisiana inner continental shelf: the 20th century record. Mar Micropaleontol 54:263–283

Raitsos DE, Yi X, Platt T, Racault M, Brewin RJW, Pradhan Y, Papadopoulos VP, Sathyendranath S, Hoteit I (2015) Monsoon oscillations regulate fertility of the Red Sea. Geophys Res Lett 42:855–862

Reyment RA, Joreskog KG (1996) Applied factor analysis in the natural sciences. Cambridge University Press, Cambridge, p 371

Rohling EJ, Fenton M, Jorissen FJ, Bertrand P, Ganssen G, Caulet JP (1998) Magnitudes of sea-level lowstands of the past 500,000 years. Nature 394:162–165

Rohling EJ, Grant KM, Roberts AP, Larrasoaña JC (2013) Palaeoclimate variability in the Mediterranean and Red Sea regions during the last 500,000 years; implications for hominin migrations. Curr Anthropol 54(No. S8, Alternative Pathways to Complexity: Evolutionary Trajectories in the Middle Paleolithic and Middle Stone Age):S183–S201

Schulz H, Rad U, Erlenkeuser H (1998) Correlation between Arabian Sea and Greenland climate oscillations of the past 110,000 years. Nature 393:54–57

Sen Gupta BK, Machain-Castillo ML (1993) Benthic foraminifera in oxygen-poor habitats. Mar Micropaleontol 20:183–201

Siccha M, Trommer G, Schulz H, Hemleben C, Kucera M (2009) Factors controlling the distribution of planktonic foraminifera in the Red Sea and implications for the development of transfer functions. Mar Micropaleontol 72:146–156

Siddall M, Smeed DA, Matthieen S, Rohling EJ (2002) Modeling the seasonal cycle of the exchange flow. Deep-Sea Res 49:1551–1569

Siddall M, Rohling EJ, Almogi-Labin A, Hemleben C, Meischner D, Schmelzer I, Smeed DA (2003) Sea-level fluctuations during the last glacial cycle. Nature 423:853–858

Siddall M, Smeed DA, Hemleben C, Rohling EJ, Schmelzer I, Peltier WR (2004) Understanding the Red Sea response to sea level. Earth Planet Sci Lett 225:421–434

Sofianos SS, Johns WE (2007) Observations of the summer Red Sea circulation. J Geophys Res 112:C06025. https://doi.org/10.1029/2006JC003886

Sofianos S, Papadopoulos V, Abulnaja Y, Giouroukou D, Bolonaki E, Hoteit I (2016) Summer-time monsoon-driven variability in the Red Sea and the effects of the exchanges with the Indian Ocean. In: International conference on the marine environment of the Red Sea. King Abdullah University of Science and Technology

Southon J, Kashgarian M, Fontugne M, Metivier B, Yim WW-S (2002) Marine reservoir corrections for the Indian Ocean and Southeast Asia. Radiocarbon 44:167–180

Thiede J (1975) Distribution of foraminifera in coastal waters of an upwelling area. Nature 253:712–714

Triantafyllou G, Yao F, Petihakis G, Tsiaras KP, Raitsos DE, Hoteit I (2014) Exploring the Red Sea seasonal ecosystem functioning using a three-dimensional biophysical model. J Geophys Res Oceans 119:1791–1811

Trommer G, Siccha M, Rohling EJ, Grant K, van der Meer MTJ, Schouten S, Hemleben C, Kucera M (2010) Millennial-scale variability in Red Sea circulation in response to Holocene insolation forcing. Paleoceanography 25. https://doi.org/10.1029/2009PA001826

Van der Zwaan GJ, Duijnstee IAP, den Dulk M, Ernst SR, Jannink NT, Kouwenhoven TJ (1999) Benthic foraminifers: proxies or problems? a review of paleoecological concepts. Earth Sci Rev 46:213–236

Weiner A, Weinkauf M, Kurasawa A, Darling K, Kucera M (2015) Genetic and morphometric evidence for parallel evolution of the *Globigerinella calida* morphotype. Mar Micropaleontol 114:19–35

Woelk S, Quadfasel D (1996) Renewal of deep water in the Red Sea during 1982–1987. J Geophys Res 101(C8):18155–18165

Wyrtki K (1974) On the deep circulation of the Red Sea. L'oceanographie physique de la Mer Rouge. Cent Natl pour l'Exploitation des Oceans, Paris, pp 135–163